Geomechanics and Engineering, *Vol. 42, No. 2 (2025) 107-116*
https://doi.org/10.12989/gae.2025.42.2.107

Kriging interpolation-based RQD prediction and engineering modeling of mineral deposits: A case study

Xingdong Zhao[a], Lei Deng* and Ye Bai[b]

School of Resources and Civil Engineering, Northeastern University, Shenyang 110819, Liaoning, China

(*Received January 13, 2025, Revised July 1, 2025, Accepted July 4, 2025*)

Abstract. Rock Quality Designation (RQD) is an important index for assessing rock mass integrity. In this paper, the RQD of geological cores drilled from geological exploration boreholes of Qinglonggou Mine is used as the basic data to analyze spatial correlations of discrete RQD borehole data through statistical methods. The mean RQD profile method was used to test the smoothness of *RQD(x)*. The normal score method was applied to transform the original *RQD(x)* data into a standard Gaussian distribution function to reduce the difference between the extremes of the original *RQD(x)* and to reduce the heteroskedasticity of the RQD. A semi-variogram model was established to characterize *RQD(x)* spatial structure in the 323-South section. Kriging interpolation method was used for RQD interpolation prediction, based on which a three-dimensional RQD model was constructed for 323-South mine section. The RQD prediction and modeling results of the 323-South section show that the spatial variability characteristics of the RQD of the 323-South section are positively correlated with the fault structure, lithology and weathering conditions.

Keywords: geological hazard modeling; geostatistics; rock mass quality prediction; RQD; spatial variability

1. Introduction

RQD in mineral deposits is one of the most important indicators to evaluate the rock engineering, and its accurate prediction is crucial to the success and safety of engineering (Liu *et al.* 2015, Liu *et al.* 2021, Yin *et al.* 2022, Zhang *et al.* 2012, Junaid *et al.* 2024a, Junaid *et al.* 2024b, Junaid *et al.* 2023). RQD prediction and engineering modeling is an important problem in geological engineering, and related research has a long history. Current methodologies for RQD prediction and engineering modeling include: statistical methods, machine learning methods, and artificial intelligence methods (Mahmoodzadeh *et al.* 2021, Murlidhar *et al.* 2021, Peng *et al.* 2021, Zhou *et al.* 2020).

RQD is the ratio (expressed as a percentage) of the cumulative length of columnar cores greater than 10 cm per run to each drillback run. Statistical methods are one of the most commonly used methods in RQD prediction of mineral deposits, which include least squares and regression analysis. These methods build RQD prediction models by performing mathematical statistical analysis on sampled data to derive prediction results. Although these methods have the advantages of simplicity and ease of use and small amount of data, their prediction accuracy is low and limited by problems such as uneven distribution of sampling points and insufficient number of samples (Alipour and Mokhtarian 2021, Hsiao *et al.* 2020, Pourhashemi *et al.* 2021, Xia *et al.* 2022). Machine learning methods are emerging methods in RQD prediction of mineral deposits in recent years, which include support vector machines and artificial neural networks. These methods can solve the problems of uneven data and insufficient quantity to a certain extent and improve the prediction accuracy by learning from a large amount of data and building prediction models. However, these methods need the support of large amount of data and computing resources, which are computationally intensive, and the interpretability of the models is low (Alzubaidi *et al.* 2022, Nanehkaran *et al.* 2022). In addition to the above methods, there are some other prediction methods, such as fuzzy mathematics and genetic algorithm. These methods can improve the prediction accuracy to a certain extent, but their applicability and effectiveness still need to be further explored (Armaghani *et al.* 2019, Hu *et al.* 2022, Tao *et al.* 2022, Xie *et al.* 2022, Zhang *et al.* 2022).

The traditional RQD prediction method suffers from the problems of insufficient sampling points, improper sampling methods, and uneven sample data, resulting in low accuracy of prediction results, which is difficult to meet the demand of engineering modeling. Therefore, the RQD prediction technology of mineral deposits based on Kriging interpolation method has become a research hotspot. Kriging interpolation method is an interpolation method based on spatial statistics, which has the advantages of high accuracy, high efficiency and independent of sampling point distribution, and can effectively improve the accuracy and reliability of RQD prediction of mineral deposits (Armaghani *et al.* 2019, Madani *et al.* 2018).

Kriging interpolation method is a spatial interpolation method based on the principle of statistics, whose basic idea

*Corresponding author, Ph.D.
E-mail: denglei635@126.com
[a]Professor
E-mail: zhaoxingdong@mail.neu.edu.cn
[b]Master Student

ISSN: 2005-307X (Print), 2092-6219 (Online)

is to analyze and model the spatial variability of the sampled data, and then predict the value of the unknown location (Aalianvari *et al*. 2018, Aziz *et al*. 2017, Kim *et al.* 2023, Masoud and Aal 2019, Ozturk and Simdi 2014). The application of Kriging interpolation method in the study of mineral deposits is relatively extensive, mainly including the following aspects: (1) deposit reserve assessment: by performing Kriging interpolation on the sampled data of mineral deposits, the ore content at unknown locations within the deposit is predicted, and then the reserve and value of the deposit are assessed. (2) Deposit Exploration: By performing Kriging interpolation on the deposit exploration data, the ore content and composition of unknown locations within the deposit are predicted, which in turn guides mine exploration and mining. (3) Deposit characterization: By performing Kriging interpolation on deposit sample data, the physical properties and geological characteristics of unknown locations within the deposit are predicted, and then the formation mechanism and evolution law of the deposit are studied in depth.

Kriging interpolation method has also been widely used in the prediction of RQD of mineral deposits. Through statistical analysis of the sampled data, Kriging interpolation model is established to make accurate prediction of the data such as RQD of the deposit. These prediction results can provide an important reference basis for mine mining and help mine mining planning and design. At the same time, Kriging interpolation method can also improve the prediction accuracy and reduce the data sampling volume and error, which has important application value.

The purpose of this paper is to develop a geostatistical framework for RQD prediction and engineering modeling of ore deposits based on Kriging interpolation method, in order to solve the shortcomings of traditional prediction methods and provide a reliable prediction and modeling basis for mine mining. This study will explore the effect of Kriging interpolation in RQD prediction and engineering modeling of mineral deposits through an in-depth discussion of the principle and application of Kriging interpolation method, combined with practical case studies, aiming to improve the safety, economy and efficiency of mineral deposit mining, which has important theoretical and practical significance.

While diverse interpolation methods exist for RQD prediction, their limitations in mining contexts warrant careful consideration:

Inverse Distance Weighting (IDW) relies solely on proximity-based weighting, ignoring spatial anisotropy critical in faulted terrains and lacking error quantification. Spline methods generate smooth surfaces but oversimplify geological discontinuities and produce edge artifacts. Artificial Neural Networks (ANN) require large datasets (>10,000 samples) for robust training and offer low interpretability of spatial weights Kriging was selected for its unique ability to: Model directional variability through semi-variograms; Quantify prediction uncertainty via Kriging variance, Preserve geologically significant boundaries, and Achieve higher accuracy with moderate-sized datasets.

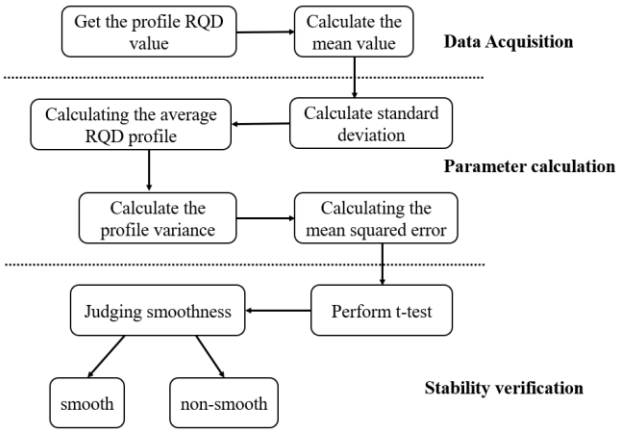

Fig. 1 RQD smoothness test flow chart

2. RQD prediction method based on Kriging interpolation

2.1 RQD smoothness assumption and data transformation

The RQD of the spatial zone of a geological exploration borehole is the determined value of the borehole location, hole depth and orientation spatial zone position x0 (x, y, z), and RQD is treated as a regionalized random variable denoted as *RQD(x)*. That is, RQD is a function related to the spatial location x of a certain exploration borehole, which varies with the spatial variability of geological formations and has spatial variability.

In order to statistically and analyze the spatial distribution pattern of *RQD(x)*, and to make an estimate of $RQD(x_i)$ in the adjacent unknown region, the assumption of smoothness of *RQD(x)* in the study area is needed. That is, the mean and variance of *RQD(x)* mainly depend on the correlation between the geological core RQD sample data on the distance h, and are independent of the data spatial location *x*. Therefore, the smoothness of *RQD(x)* in the region needs to be tested before modeling with the semi-variance function.

This was done by taking a number of parallel lines at equal distance intervals on a selected rock plane. For each parallel line, the RQD values along the line direction are measured in the usual way and the average value is calculated. The average value of each parallel line forms a series, and then the smoothness test is performed on this series (Fig. 1). This test determines whether the series is statistically stationary. If the series is smooth, its statistical properties do not change over time and can be applied in areas such as time series analysis and forecasting. The smoothness test of *RQD(x)* using the average RQD profile method can improve the reliability and accuracy of rock engineering design, thus better ensuring the stability and safety of the rock mass.

Heteroskedasticity indicates unequal variances in RQD measurements across spatial locations, i.e., the inconsistent size of data fluctuations. To describe the variation of RQD(x) in space, it can be described by the mean and variance of RQD(x). Therefore, assuming that RQD(x) obeys a Gaussian

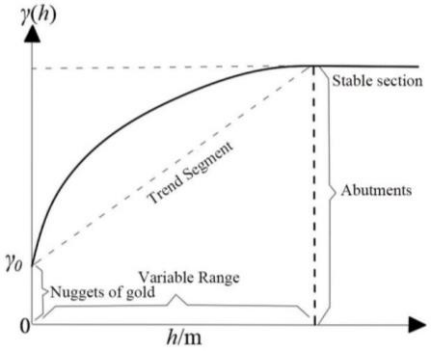

Fig. 2 Semi-variable function of *RQD(x)*

distribution, the original RQD(x) data can be transformed into the standard Gaussian distribution function $RQD_{Nor(x)}$ using the normal score method. The effect of this method is to effectively reduce the difference between the extreme values of *RQD(x)*, while reducing the heteroskedasticity in the RQD data.

The normal score transformation maps raw *RQD(x)* data onto a standard Gaussian distribution, which eliminates the heteroskedasticity and skewness between the data and makes the data more consistent with the assumption of a normal distribution. In the normal score method, the data are standardized by calculating the mean and standard deviation of the original data, and then the normal distribution function is used to find the corresponding quantile to obtain the transformed standard normal distribution data.

2.2 Semi-variance function analysis

To link the traditional statistical characteristics (mean *m*, variance σ^2) to spatial locations and to study the spatial correlation properties of the regionalized random variable *RQD(x)* at different locations *x* and *x+h*, the self-covariance function *C(h)* is introduced as follows

$$\begin{aligned} C(h) &= cov[RQD(x),(x+h)] \\ &= E[RQD(x)RQD(x+h)] - m^2 \end{aligned} \quad (1)$$

The variance function is a tool for structural analysis of regional variables and a means of describing the non-homogeneity of the object of study. The variation function $\gamma(h)$ is defined as the variance of the increment of the regional variation.

$$\gamma(h) = \frac{1}{2}E\{[Z(X+h) - Z(X)]^2\} \quad (2)$$

Where: $Z(X)$ and $Z(X+h)$ are the variation of two regions at a location *X* and h away from it in space, respectively. Usually, the variogram cloud is obtained by plotting the distance between two points and the variation value as the horizontal and vertical axes. Then the variogram cloud is divided into several groups by setting the lag distance, and finally the average variation function value is calculated, i.e., the experimental variation function $\gamma^*(h)$is used to estimate $\gamma(h)$, the specific formula is

$$\gamma^*(h) = \frac{1}{2N(h)}\sum_{i=1}^{N(h)}[Z(X_i+h) - Z(X_i)]^2 \quad (3)$$

Where: h is the lag distance; $N(h)$is the number of data pairs corresponding to lag distance h; $Z(X_i)$, $Z(X_i+h)$ are the measured values of $X_i$and X_i+h points, respectively.

The *RQD(x)* semi-variance function is characterized by three parameters: the block gold value γ_0, the abutment value *C*, and the variation range *h* (Fig. 2), which is the key function reflecting the spatial variability and correlation of the RQD (Fig. 2).

Assuming that RQD is *RQD(x)* at a point x in a geological borehole space, the correlation between *RQD(x)* and *RQD(x+h)* can be expressed as

$$\begin{aligned} \gamma(h) &= \frac{1}{2}Var[RQD(x) - RQD(x+h)] \\ &= \frac{1}{2}E[RQD(x) - RQD(x+h)]^2 \end{aligned} \quad (4)$$

Under the smoothness assumption, the semi-variance function of *RQD(x)* in the study area can be obtained from the average estimate of *RQD(xi)* for known data.

$$\gamma^*(h) = \frac{1}{2N(h)}\sum_{i=1}^{N(h)}\left[RQD(x_i) - RQD(x_i+h)\right]^2 \quad (5)$$

where, *N(h)* is the number of all point pairs at distance *h* in the study area, and *RQD(xi)* denotes the RQD value at the location.

2.3 Principle of Kriging interpolation method

In this paper, Kriging interpolation is used to interpolate the prediction of the adjacent unknown region RQD. Kriging interpolation has linear, unbiased and optimal estimation properties. In addition, Kriging explicitly corrects prediction bias induced by irregular data clustering. The principle of Kriging interpolation is as follows

Let $RQD(x_1),\ldots,RQD(x_n)$ be a set of known data near the location to be predicted, then the estimated value of *RQD*(x₀)* at the location can be estimated by a linear combination of known data

$$RQD^*(x_0) = \sum_{i=1}^{n}\lambda_i RQD(x_i) \quad (6)$$

where the weight coefficients are given by the unbiasedness and optimality conditions, and to ensure the unbiasedness of *RQD*(x₀)*, set

$$\sum_{i=1}^{n}\lambda_i = 1 \quad (7)$$

To ensure optimality then the error variance of *RQD*(x₀)* is minimized

$$\begin{aligned} S = Min\{Var[RQD(x_0) - RQD^*(x_0)]\} \\ = Min\{Var(RQD(x_0) \\ - 2\sum_{i=1}^{n}\lambda_i\, cov[RQD(x_i), RQD(x_0)] \\ + \sum_{i=1}^{n}\sum_{j=1}^{n}\lambda_i\lambda_j\, cov[RQD(x_i), RQD(x_j)]\} \end{aligned} \quad (8)$$

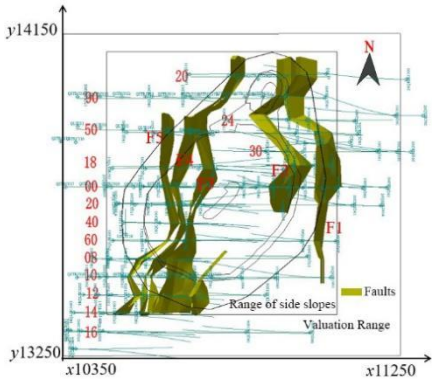

(a) Drill hole location map

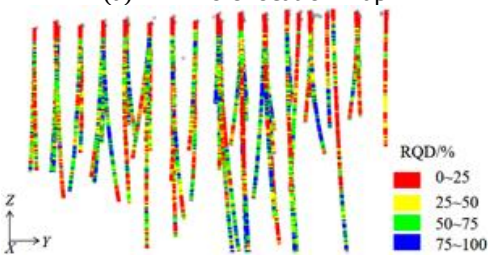

(b) Drill hole space distribution map

Fig. 3 Location and spatial distribution of geological survey boreholes in the 323-South section

where $cov[RQD(x_i), RQD(x_j)]$ is the covariance of the two points, and $RQD^*(x_0)$ is obtained by solving Eqs. (6)-(8) jointly, at which point S is said to be the Kriging variance.

To solve for the minimum error variance S, i.e., to find the minimal value of Eqs. 8 under Eqs. (7), introduce the Lagrange factor φ, construct the function to derive and have

$$\begin{cases} \frac{\partial[2\sum_{i=1}^{n}\lambda_i\gamma(x_i-x_0)-\sum_{i=1}^{n}\sum_{j=1}^{n}\lambda_i\lambda_j\gamma(x_i-x_j)-2\varphi(\sum_{i=1}^{n}\lambda_i-1)]}{\partial\lambda_j}=0 \quad j=1,2,\cdots n \\ \frac{\partial[2\sum_{i=1}^{n}\lambda_i\gamma(x_i-x_0)-\sum_{i=1}^{n}\sum_{j=1}^{n}\lambda_i\lambda_j\gamma(x_i-x_j)-2\varphi(\sum_{i=1}^{n}\lambda_i-1)]}{\partial\varphi}=0 \end{cases} \tag{9}$$

That is

$$\sum_{i=1}^{n}\lambda_i\gamma(x_i-x_j)+\varphi=\gamma(x_i-x_j) \qquad \sum_{i=1}^{n}\lambda_i=1 \tag{10}$$

Written in matrix form as

$$\begin{vmatrix} \gamma_{11} & \cdots & \gamma_{1n} & 1 \\ \vdots & & \vdots & \vdots \\ \gamma_{n1} & \cdots & \gamma_{nn} & 1 \\ 1 & \cdots & 1 & 0 \end{vmatrix} \begin{vmatrix} \lambda_1 \\ \vdots \\ \lambda_n \\ \varphi \end{vmatrix} = \begin{vmatrix} \gamma_{01} \\ \vdots \\ \gamma_{0n} \\ 1 \end{vmatrix} \tag{11}$$

3. Project example

3.1 Project overview

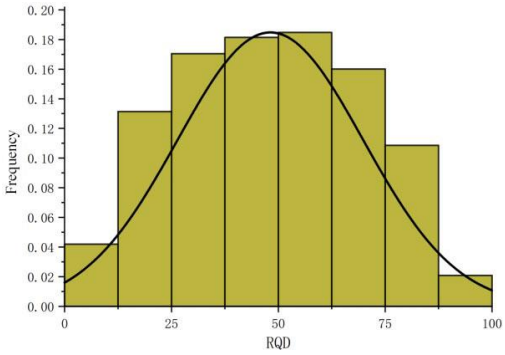

Fig. 4 RQD distribution histogram of engineering exploration drilling in 323S mine

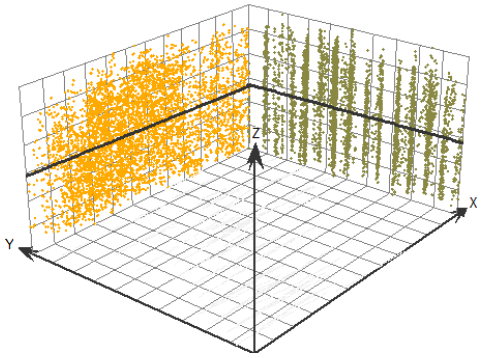

Fig. 5 Trend analyses of RQD

The Qinglonggou mine (Qinghai Province, China) is situated approximately 95 km northwest of Dachaidan, its 323-South section of the mine coordinates range: X: 10350-11250 m, Y: 13250-14150 m, Z: 3250-3550 m, the mine area range is 900m long and wide each, the ore body buried above the level of 3250 m, the depth is about 300 m. The geological exploration borehole network degree is 40m×40m (Fig. 3(a)), and the number of geological boreholes is 126, of which 118 geological boreholes counted RQD values (Fig. 3(b)), and the cumulative number of RQD groups counted is 4,457 groups. Fig. 4 shows that RQD values predominantly range between 25–75%, accounting for 66% of observations

3.2 Stability assumptions and data transformations

Based on 323 South geological borehole location, hole depth and orientation, a three-dimensional model of 323 South geological borehole RQD is established (Fig. 3(b)). The RQD of a certain geological exploration borehole spatial section is the determined value of borehole location, hole depth and orientation spatial section location $x_0(x, y, z)$, and the RQD is defined as a regionalized random variable $RQD(x)$, that is, the RQD is a function related to a certain exploration borehole spatial location x, which varies with the geological structure spatially and has spatial variability. In this paper, the mean RQD profile method is used to test the smoothness of $RQD(x)$. The average RQD profile method is a method to test the smoothness of $RQD(x)$. The basic idea is to average multiple RQD values of the sampled line and use the average value along the length of the rock

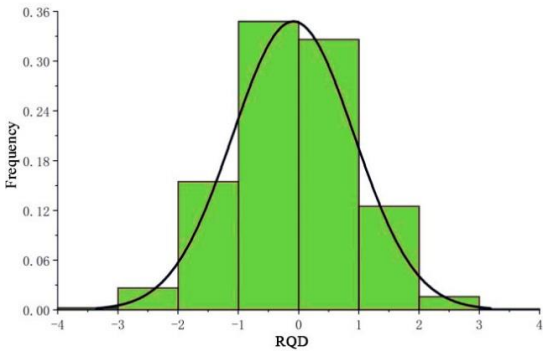

Fig. 6 Histogram of normal transformation scores

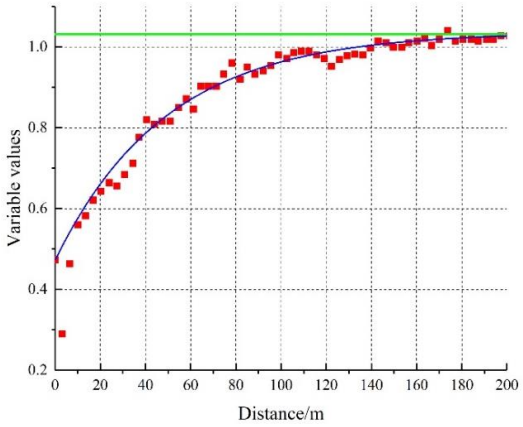

Fig. 7 Omnidirectional semi-variable function (*h*=3 m)

as a new series, and then test whether this series is smooth by statistical methods. The results are shown in Fig. 5.

To address heteroskedasticity in *RQD(x)*, assuming that *RQD(x)* obeys Gaussian distribution, the characteristics of *RQD(x)* at any position x in space can be described by the mean and variance of *RQD(x)*. The normal score method is used to transform the original *RQD(x)* data into the standard Gaussian distribution function $RQD_{Nor}(x)$ (Fig. 6), which effectively reduces the difference between the extreme values of *RQD(x)* and also reduces the heteroskedasticity in the *RQD* data.

3.3 Semi-variance function analysis

By establishing the horizontal omnidirectional semi-variance function of *RQD(x)* of the geological borehole (Fig. 7) and the semi-variance function along the orientation of the geological borehole (Fig. 8). From Figs. 7 and 8, it can be seen that both the horizontal omnidirectional semi-variance function of the geological borehole and the semi-variance function along the borehole orientation have obvious trend-up and smooth segments. The fit is basically consistent with the *RQD(x)* theoretical semi-variance function (Fig. 2), which has good spatial structure in the whole.

Owing to mineralization mechanisms and geological structures of the rock mass in the 323 South section, the *RQD(x)* has different continuity in each direction, which leads to the anisotropy of the *RQD(x)* semi-variance function. In this paper, we only consider the geometric

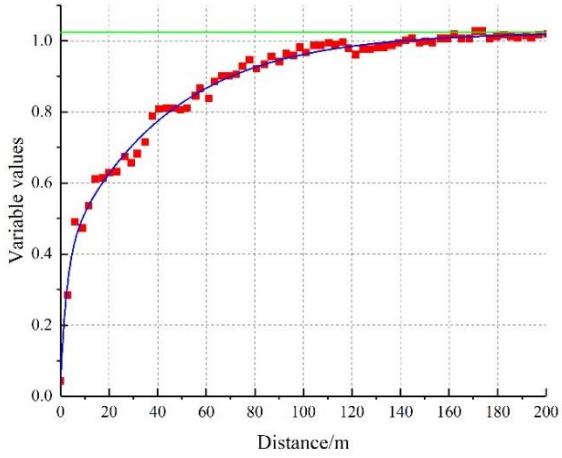

Fig. 8 Downhole semi-variable function (*h*=3 m)

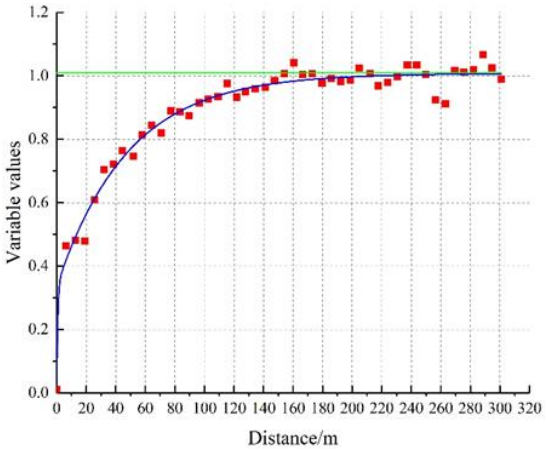

(a) Azimuth 22.5°, inclination 0°，*h*=3 m

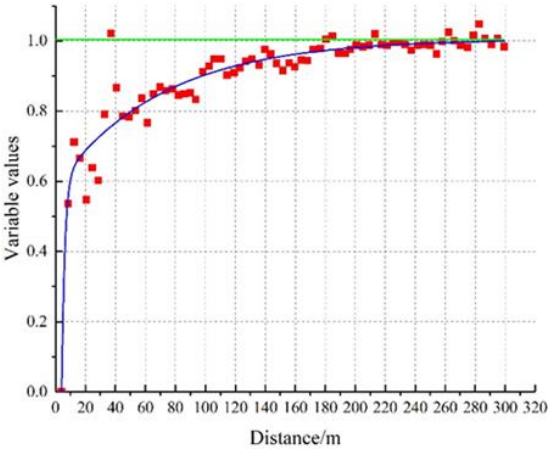

(b) Azimuth 172.55°, inclination -45°，h=3 m

Fig. 9 Theoretical semi-variable function in different directions

anisotropy of the semi-variance function, that is, the semi-variance function has the same block gold value γ_0 and different variation h in different directions, and characterize its geometric anisotropy by the ratio of the variation in each axis direction. Meanwhile, the *RQD(x)* sample data present a non-uniform and irregular distribution, which constrains the direction and range of searching $RQD(x_i)$ sample data point pairs to obtain the priority sampling data point pairs.

Table 1 Parameters of theoretical semi-variable function

Angle	Theoretical model	Nugget Value	Abutment value	Variable range/m
Azimuth 22.5°, inclination 0°	Index Model	0.40	0.58	160
Azimuth 165°, inclination 45°	Index Model	0.40	0.56	140

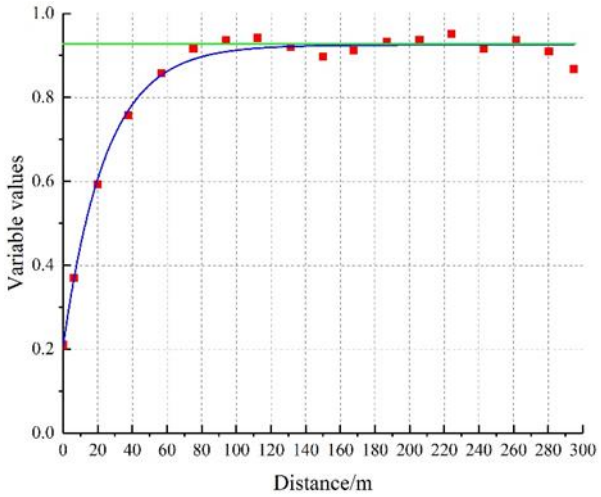

Azimuth 300°, inclination -45°，h=12 m
Fig. 10 Secondary semi-variogram

In order to quantitatively characterize the spatial structure of *RQD(x)* in the mine area, the maximum continuity direction of *RQD(x)* needs to be determined first, mainly considering the spatial structure of parameters and variables related to the horizontal and vertical directions of geological boreholes through geological bodies and structures. In this paper, two main planes of inclination 0° and -45° are selected based on the design angle of geological drill holes in the 323-South section of Qinglonggou Mine. In each main plane, the constrained cone search body was used to analyze the continuity of *RQD(x)* in different orientations and obtain the optimal continuity orientation in the two main planes (Fig. 9).

The ideal *RQD(x)* semi-variance function should have a smaller block gold value γ0 and a larger variation range h. According to the analysis results of the RQD semi-variance function of the actual geological exploration borehole on site (see Table 1), it can be seen that RQD has a larger variation range in the direction of azimuth 22.55° and dip 0°, so the direction is set as the main axis direction.

After determining the *RQD(x)* principal axis direction and semi-variance function, the best semi-variance function of the secondary axis was obtained by observing different secondary axis directions and continuously adjusting the step h to obtain the best semi-variance function of the secondary axis, and adjusting the ratio of the *RQD(x)* principal axis variation to the secondary axis variation to make the best fit of the theoretical semi-variance function in the secondary axis direction (Fig. 10). The short-axis direction is perpendicular to the maximum continuity plane where the major axis and the minor axis are located. By continuously adjusting the step h in the short-axis direction

Table 2 Anisotropic structural parameters

Parameters	Spindle azimuth	Spindle tilt angle	Secondary axis tilt angle	Primary/secondary axis	Primary/ short axis
Value	22.5°	0°	-45°	1.26	1.41

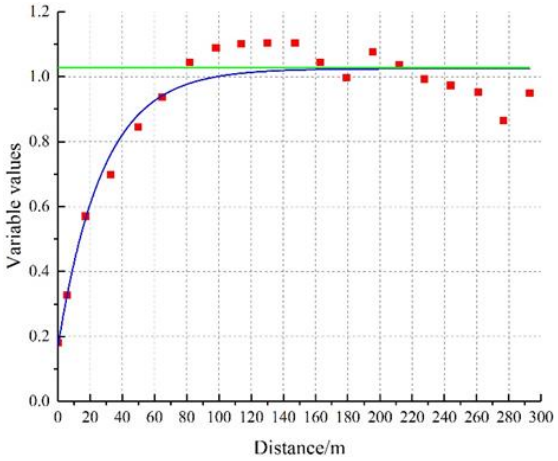

Azimuth 120°, inclination -45°，h=12 m
Fig. 11 Minor semi-variable function

and the ratio of the major axis variation to the short-axis variation, the theoretical semi-variance function of *RQD(x)* also achieves the best fit in the short-axis direction (Fig. 11).

It can be seen in the Table 2 that the theoretical semi-variance functions are better structured in the major axis and minor axis directions, while slightly less structured in the short axis direction, which is mainly due to the complex geological formations in the region that affect the spatial structure of RQD.

3.4 Kriging interpolation RQD 3D prediction modeling

The block model was established in 3DMine software. Since the vertical depth of open pit mining in the 323-South section is 300 m, the horizontal length and width are 900 m each, the height of the open pit step is 12 m, and the length of the drill hole return is 3 m. In order to accurately characterize the spatial distribution of RQD in the 323 South section, the block was set to 6 m × 6 m × 3 m, with a total of 2.3 × 10^6 units. To ensure the local accuracy of the RQD model, ordinary Kriging was used for *RQD* interpolation of the block; the block RQD semi-variance function and anisotropic structure parameters are shown in Tables 1 and 2. For the number of sample points constraint, a minimum of 3 sample points and a maximum of 12 sample points are taken for each cell valuation. The RQD 3D predicted block model was obtained by adding surface, side slope extent and mining pit DTM for constraint display (Fig. 12). From Fig. 12, it can be seen that the rock masses in the near-surface layer of the 323 South section exhibit rock fragmentation and incompleteness, while the rock integrity is better in the deeper part of the mining pit exposures.

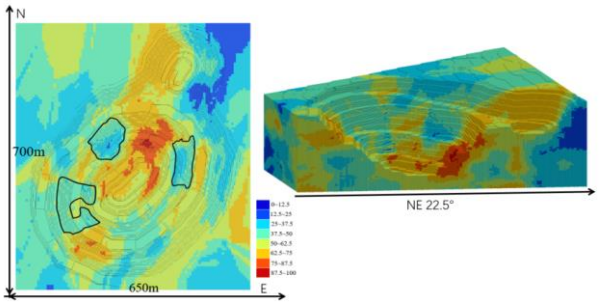

Fig. 12 RQD estimation 3D model

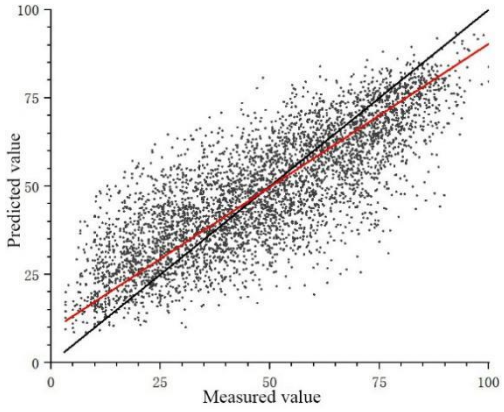

Fig. 13 Kriging cross validation results

Table 3 Performance indicators of Kriging estimation

Number of samples/pc	Root Mean Square Error/RMSE	Correlation coefficient/ R^2	Regression slope/k
4457	14.12	0.69	0.83

3.4.1 Model validation and evaluation

In order to check the accuracy of the Kriging interpolation RQD 3D prediction model, this paper uses the cross-validation method for verification. The RQD at a known location in the RQD 3D prediction model is first hidden, and then the estimated RQD at that location is calculated from other known RQD by Kriging interpolation prediction. Predicted RQD values were compared with measured values to quantify accuracy. The textbook cross-validation comparison was performed for all RQD sample points. The cross-validation results are shown in Fig. 13, where the black color is the RQD true value curve and the red color is the least squares regression line of the RQD interpolated predicted value, and the deviation values of the two are small. The corresponding regression parameters are shown in Table 3.

where the root mean square error of RQD prediction is

$$RMSE = \sqrt{\frac{\sum_{i=1}^{N}(RQD(x_i) - RQD^*(x_i))^2}{N}} \quad (12)$$

Where $RQD(x_i)$ indicates the true value of RQD at the point and $RQD(x_i)^*$ is the predicted value of RQD at the point, according to which the RQD 3D prediction model established by the calculation has a prediction accuracy of 70% on the whole.

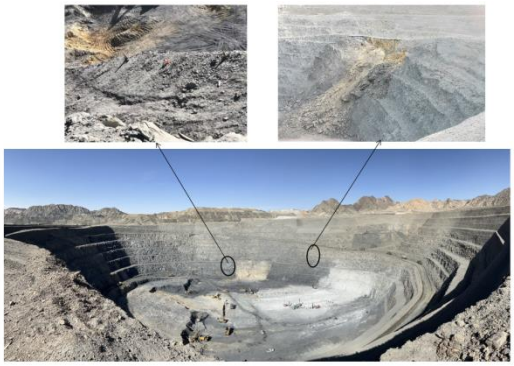

Fig. 14 Instability of the west wall in 323 South mine

3.4.2 323 South mine section excavation slope verification

According to the RQD three-dimensional prediction model, it can be seen that the RQD of the 323 South section shows a certain striped distribution on the whole (Fig. 14). The RQD has small variability and strong continuity in the north-south direction, while it has large variability and poor continuity in the east-west direction. Meanwhile, RQD shows non-uniformity locally and has a significant spatial clustering effect. By adding constraints such as ground surface in Fig. 14, the prediction model of 323 South section is made consistent with the actual mine mining 3D model, and the side slopes of 323 South open pit are progressively excavated and exposed based on the open pit mining sequence of 323 South section. In the RQD 3D prediction model in Fig. 12, a large area of low-quality rock (RQD=0-25%) appears in the eastern northern side gang and the western local side gang of the open pit in the 323 South section. Also, in Fig. 14, a slope slide and a large fracture occurred in the western side gang of the mining area, which is consistent with the potential landslide area (poor quality rock side gang) revealed by the RQD model. It can be seen that the RQD 3D prediction model can identify and judge the spatial location of potential poor-quality engineered rock bodies (RQD=0-25%) in the mining area, and can over-judge the location of unstable slopes and provide basic information for slope stability control and support reinforcement.

3.4.3 RQD variation characterization

Based on the fault data of the 323 South section and field site investigation data, the geological structure model of the 323 South section of the Qinglonggou gold mine was established through the solid modeling module in 3DMine, and the cross-sectional RQD cloud map was obtained through the tangential RQD 3D prediction block model (Fig. 15). Due to the low RQD value of the fault structure (below 50%), the distribution of the fault structure and its orientation can be clearly seen, which controls the main spatial variation characteristics of the RQD 3D prediction model of the 323 South section.

Different rock types usually have different physical and mechanical properties. The rock types in the 323 South section mainly include shallow metamorphic rocks (kilohertz, schist), carbonate rocks (dolomite), and hard

Table 4 RQD statistical indicators of different types of rock masses

Rock type	Dolomite	Gabbro	Metamorphic amphibolite	Schist	Chimei Rock	Sandstone	Quaternary sediments
RQD Mean Value	63	57	61	38	42	31	5
Cumulative length/m	1300	1045	994	2558	2933	382	1500
Standard deviation	22	24	19	21	23	13	0.6
Coefficient of variation/c_v	0.32	0.39	0.31	0.55	0.54	0.42	0.12

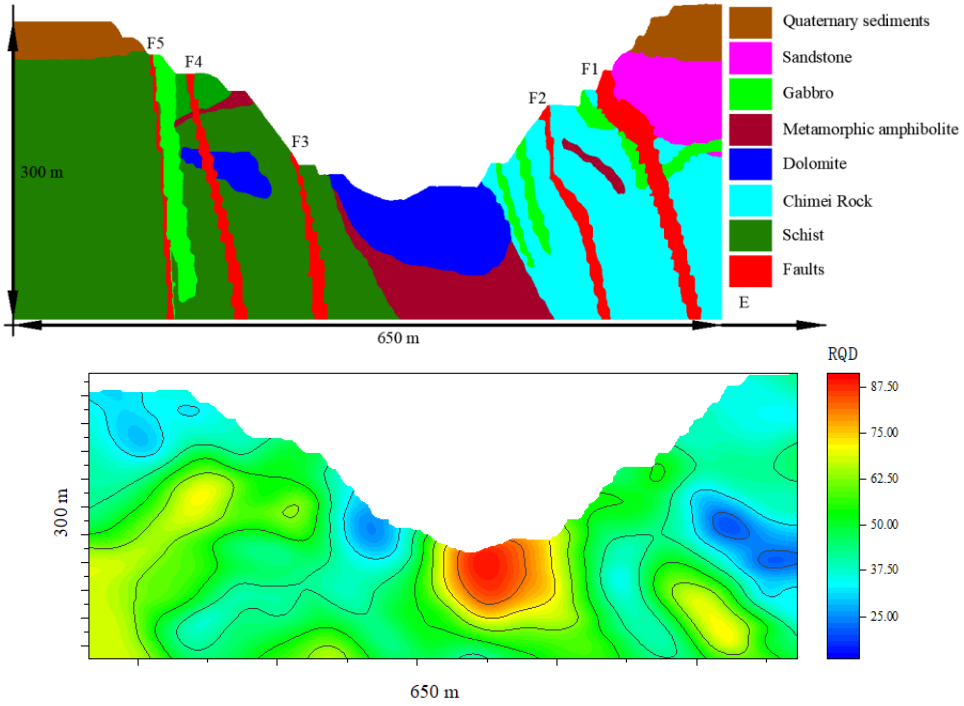

Fig. 16 Geological profile and RQD distribution cloud map of exploration line 18

intrusive rocks (meta diorite and gabbro). The geological profile was obtained by delineating and circling the lithologic divisions in the drill hole section of the 18-exploration line (see Fig. 3(b) for location), and the RQD distribution cloud map was obtained by cutting the 3D block model. The RQD distribution in the same lithological section of the original drill hole of the mining pit was obtained and statistically analyzed by the section circling module (Table 4).

As shown in Table 4 and Fig. 16, the spatial variability of RQD varies between different lithologies. 323 South section is composed of schist and schist in the east and west, and the original rocks are mainly carbonate, siliceous and mudstone. The integrity of the rocks is poor due to the geological structure and weathering, while the deep carbonate dolomite and metamorphic rocks have better integrity due to the hardness of the rocks and the distance from the tectonic zone, with RQD values above 60%. The above analysis indicates that the spatial variability of the RQD 3D prediction model is the result of the combined effect of geotectonic activity and weathering conditions.

4. Conclusions

In this paper, we apply geostatistical methods to analyze and model the spatial structure of RQD data from geological exploration drill holes in the 323 South section of the Qinglonggou gold mine, and draw two conclusions as follows.

- The mean RQD value (48.15) indicates moderately fractured rock in the 323-South section. The coefficient of variation is 0.45, which has a medium degree of variation. The semi-variance function analysis indicates that the RQD has good spatial structure. RQD spatial variability is primarily controlled by geological structures (faults), lithology, and weathering intensity.
- Kriging interpolation was used to construct the RQD 3D predictive block model of the 323 South section to predict and characterize the spatial distribution of rock quality RQD in the 323 South section. The model successfully identified low-RQD zones (0–25%) corresponding to actual slope failures.

Acknowledgments

This work was supported by the Key projects of National Natural Science Foundation of China (52130403). The authors' special thanks go to CSC (China Scholarship Council) for the scholarship (CSC Student ID: 202106080060).

References

Aalianvari, A., Soltani-Mohammadi, S. and Rahemi, Z. (2018), "Estimation of geomechanical parameters of tunnel route using geostatistical methods", *Geomech. Eng.*, **14**(5), 453-458. https://doi.org/10.12989/gae.2018.14.5.453.

Alipour, A. and Mokhtarian, M. (2021), "RSM-based model to estimate the V-cut drill and blast pattern specific charge in rock tunneling", *Int. J. Geomech.*, **21**(11), 6021030. https://doi.org/10.1061/(ASCE)GM.1943-5622.0002180.

Alzubaidi, F., Mostaghimi, P., Si, G.Y., Swietojanski, P. and Armstrong, R.T. (2022), "Automated rock quality designation using convolutional neural networks", *Rock Mech. Rock Eng.*, **55**(6), 3719-3734. https://doi.org/10.1007/s00603-022-02805-y.

Armaghani, D.J., Koopialipoor, M., Marto, A. and Yagiz, S. (2019), "Application of several optimization techniques for estimating TBM advance rate in granitic rocks", *J. Rock Mech. Geotech.*, **11**(4), 779-789. https://doi.org/10.1016/j.jrmge.2019.01.002.

Aziz, M., Khan, T.A. and Ahmed, T. (2017), "Spatial interpolation of geotechnical data : A case study for multan city, Pakistan", *Geomech. Eng.*, **13**(3), 475-488. https://doi.org/10.12989/gae.2017.13.3.475.

Hsiao, C.C., Topacio, A.J. and Chen, Y.J. (2020), "Evaluation of side resistance for drilled shafts in rock sections", *Geomech. Eng.*, **21**(6), 503-511. https://doi.org/10.12989/gae.2020.21.6.503.

Hu, J.H., Zhou, T., Ma, S.W., Yang, D.J., Guo, M.M. and Huang, P.L. (2022), "Rock mass classification prediction model using heuristic algorithms and support vector machines: A case study of chambishi copper mine", *Sci. Rep-Uk*, **12**(1). https://doi.org/10.1038/s41598-022-05027-y.

Junaid, M., Abdullah, R.A., Abdelrahman, K., Ullah, A., Mahmood, S., Saari, R. and Islam, A. (2024), "Assigning resistivity values to rock quality designation indices using integrated unmanned aerial vehicle and 2D electrical resistivity tomography in granitic rock", *Geocarto Int.*, **39**(1), 2343019. https://doi.org/ 10.1080/10106049.2024.2343019.

Junaid, M., Abdullah, R.A., Ullah, A., Saari, R., Mahmood, S., Rehman, H., Rehman, S.U. and Sari, M. (2025), "Discontinuity characterization for slope stability assessment using combined aerial photogrammetry, and geophysics approach", *Nat. Hazards*, **121**(3), 3581-3600. https://doi.org/10.1007/s11069-024-07051-9.

Junaid, M., Abdullah, R.A., Saari, R., Shah, K.S. and Ullah, R. (2023), "A comparative study of the influence of volumetric joint counts (Jv) and resistivity on rock quality designation (RQD) using multiple linear regression", *Pure Appl. Geophys.*, **180**(6), 2351-2368. https://doi.org/ 10.1007/s00024-023-03260-8.

Kim, M., Chung, C., Han, J. and Kim, H. (2023), "Three-dimensional geostatistical modeling of subsurface stratification and Spt-N value at dam site in South Korea", *Geomech. Eng.*, **34**(1), 29-41. https://doi.org/10.12989/gae.2023.34.1.029.

Liu, F., Liu, Y., Yang, T., Xin, J.C., Zhang, P.H. and Dong, X. (2021), "Meticulous evaluation of rock mass quality in mine engineering based on machine learning of core photos", *Chin. J. Geotech. Eng.*, **43**(5), 968-974. https://doi.org/10.11779/CJGE202105023.

Liu, Y., He, S., Wang, D. and Li, D. (2015), "RQD Prediction method of engineering rock mass based on spatial Interpolation", *Rock Soil. Mech.*, **36**(11), 3329-3336. https://doi.org/10.16285/j.rsm.2015.11.039.

Madani, N., Yagiz, S. and Adoko, A.C. (2018), "Spatial mapping of the rock quality designation using multi-gaussian kriging method", *Minerals-Basel*, **8**(11). https://doi.org/10.3390/min8110530.

Mahmoodzadeh, A., Mohammadi, M., Ali, H., Abdulhamid, S.N., Ibrahim, H.H. and Noori, K. (2021), "Dynamic prediction models of rock quality designation in tunneling projects", *Transp. Geotech.*, **27**(2), 100497. https://doi.org/10.1016/j.trgeo.2020.100497.

Masoud, A.A. and Aal, A. (2019), "Three-dimensional geotechnical modeling of the soils in Riyadh City, Ksa", *B Eng. Geol. Environ.*, **78**(1), 1-17. https://doi.org/10.1007/s10064-017-1011-x.

Murlidhar, B.R., Nguyen, H. and Rostami, J., Bui, X., Armaghani, D., Rogam, P. and Mohamad, E.T. (2021), "Prediction of flyrock distance induced by mine blasting using a novel Harris Hawks optimization-based multi-layer perceptron neural network", *J. Rock Mech. Geotech.*, **13**(6), 1413-1427. https://doi.org/10.1016/j.jrmge.2021.08.005.

Nanehkaran, Y.A., Zhu, L.C., Chen, J.D., Azarafza, M. and Mao, Y.M. (2022), "Application of artificial neural networks and geographic information system to provide hazard susceptibility maps for rockfall failures", *Environ. Earth Sci.*, **81**(19), 475. https://doi.org/10.1007/s12665-022-10603-6.

Ozturk, C.A. and Simdi, E. (2014), "Geostatistical investigation of geotechnical and constructional properties in Kadikoy-Kartal subway, Turkey", *Tunn. Undergr. Sp. Tech.*, **41**(2014), 35-45. https://doi.org/10.1016/j.tust.2013.11.002.

Peng, K., Zeng, J., Armaghani, D.J., Hasanipanah, M. and Chen, Q.S. (2021), "A novel combination of gradient boosted tree and optimized ann models for forecasting ground vibration due to quarry blasting", *Nat. Resour. Res.*, **30**(6), 4657-4671. https://doi.org/10.1007/s11053-021-09899-1.

Pourhashemi, S.M., Ahangari, K., Hassanpour, J. and Eftekhari, S.M. (2021), "Evaluating the influence of engineering geological parameters on TBM performance during grinding process in limestone strata", *B Eng. Geol. Environ.*, **80**(4), 3023-3040. https://doi.org/10.1007/s10064-021-02134-4.

Tao, K., Wang, Q., Wang, H.M., Liu, T.J., Yue, D. and Wang, L.H. (2022), "An automatic fuzzy monitoring method of underground rock moisture permeation damage based on mae fractal", *Measurement*, **205**(2022), 112181. https://doi.org/10.1016/j.measurement.2022.112181.

Xia, K.Z., Chen, C.X., Wang, T.L., Pang, H.S. and Liu, X.T. (2022), "Quantification of the GSI and D values in the Hoek-Brown criterion using the Rock Quality Designation (RQD) and discontinuity Surface Condition Rating (SCR)", *B Eng. Geol. Environ.*, **81**(1), 4. https://doi.org/10.1007/s10064-021-02493-y.

Xie, H.Y., Dong, J.J., Deng, Y. and Dai, Y.W. (2022), "Prediction model of the slope angle of rocky slope stability based on random forest algorithm", *Math. Probl. Eng.*, **110**(2022), 338-366. https://doi.org/10.1155/2022/9441411.

Yin, X., Gao, F., Liu, Q., Wang, X., Huang, X. and Pan, Y. (2022), "Multi-algorithm fusion-optimization model and its engineering application for boreability evaluation of tunnel boring Machine". *Chin. J. Rock Mech. Eng.*, **41**(1), 2757-2771. https://doi.org/10.13722/j.cnki.jrme.2021.0591.

Zhang, D.B., Chu, Z.W. and Gui, Q.J., Wu, F., Yang, H., Ma, Y. and Tao, W. (2022), "Transformer maintenance decision based on condition monitoring and fuzzy probability hybrid reliability assessment", *IET Gener Transm. Dis.*, **17**(4), 976-992.

http://doi.org/10.1049/gtd2.12718.
Zhang, W., Chen, J., Yuan, X. and Ma, J. (2012), "Study of size effect and spatial effect of RQD for rock masses based on three-dimensional fracture network", *Chin. J. Rock Mech. Eng.*, **31**(7), 1437-1445. https://doi.org/10.3969/j.issn.1000-6915.2012.07.017
Zhou, J., Bejarbaneh, B.Y., Armaghani, D.J. and Tahir, M.M. (2020), "Forecasting of TBM advance rate in hard rock condition based on artificial neural network and genetic programming techniques", *B Eng. Geol. Environ.*, **79**(4), 2069-2084. https://doi.org/10.1007/s10064-019-01626-8.

CC